

GEOTECHNICAL ISSUES IN THE ANALYSIS OF MASONRY ARCH BRIDGES

Colin C. Smith^{*}, Matthew Gilbert^{*} and Philip A. Callaway^{*}

^{*} Department of Civil and Structural Engineering
University of Sheffield
Sir Frederick Mappin Building, Mappin Street,
Sheffield, S1 3JD, UK.

email: c.c.smith@sheffield.ac.uk - Web page: <http://www.shef.ac.uk/civil/staff/ccs.html>

Key words: Ultimate limit state, serviceability limit state, assessment, Eurocode, soil, backfill, load dispersal, passive resistance.

Abstract. *It has been demonstrated that the load-deflection response of a masonry arch bridge may often be primarily a function of the soil response. Consequently, and particularly given the current lack of rational and widely accepted serviceability criteria for masonry arch bridges, this paper explores an approach for estimating serviceability soil pressures on a masonry arch and thus a serviceability load capacity. Since bridge assessment engineers must consider both serviceability and ultimate limit states, the possibility of applying the relevant principles from Eurocode 7 to masonry arch bridges is examined. Parametric studies on a sample arch with cohesionless backfill indicate that stability may be controlled by either the serviceability limit state or ultimate limit state, depending on the backfill strength. In comparison, the current UK standard for the Assessment of Highway Bridges and Structures, BD21, appears to be overconservative for lower strength backfills.*

1 INTRODUCTION

Given the current lack of rational and widely accepted serviceability criteria for masonry arch bridges, this paper explores an approach for estimating serviceability soil pressures on a masonry arch and thus a serviceability load capacity. Since bridge assessment engineers must consider both serviceability and ultimate limit states, the possibility of applying the relevant principles from the geotechnical Eurocode EC7ⁱ to masonry arch bridges is examined. Calculations performed using the RINGⁱⁱ masonry arch bridge analysis software are used to compare estimated serviceability limit states (SLS) with predicted ultimate limit states (ULS). These are further compared with the approach used in the current UK code, BD21ⁱⁱⁱ.

This paper considers a plane strain analysis of an arch plus backfill and no account is taken of the contribution of spandrel walls etc. to the arch strength, or of 3D loading patterns. Consequentially the approach described will in general lead to conservative results.

2 SOIL ARCH INTERACTION

2.1 Components of soil-arch interaction

Although the principles are transferable to other failure modes, for sake of simplicity the classic four hinge soil-arch interaction model depicted in Figure 1 is considered here. Traditionally the interaction has been assumed to comprise of two independent components: (i) transference of the applied load to the arch (in the region of hinge B in Figure 1); (ii) passive resistance as the collapsing arch moves into the backfill (in the region of hinge C in Figure 1). The dead weight of the backfill also plays an important role in enhancing arch stability. Discussion will be limited to cohesionless uniform backfill (i.e. consideration of cohesive backfill & the beneficial effects of road surfacing are beyond the scope of the paper).

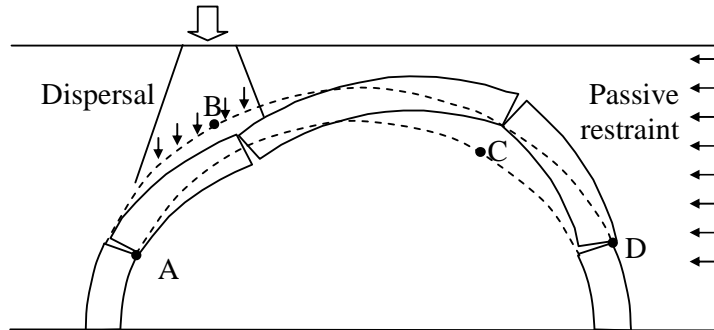


Figure 1: Masonry bridge soil-structure interaction

In order to identify the contribution of each aspect of the interaction, it is useful to examine various soil-arch interaction scenarios, starting from extremely conservative assumptions about the interaction and moving towards the more realistic models currently in use. These scenarios, listed in Table 1, may be subdivided into two classes: (i) SLS, where the assumptions imply negligible arch movement - and therefore may be considered a lower bound estimate of the Serviceability Limit State; (ii) ULS, where large deformations are

assumed and therefore may be considered to represent the Ultimate Limit State. In the case of ULS1 identified in the Table, a gross displacement analysis should ideally be employed^{iv} although since results from such an analysis will often be quite similar to those from a conventional analysis, this has not been performed for the purposes of this paper.

Scenario	Simple description
SLS1	Load capacity of bare masonry arch only.
SLS2	Load capacity of arch including effect of backfill dead weight. No load dispersal.
SLS3	At rest horizontal earth pressures included as additional load on arch.
SLS4	Effect of load dispersal through backfill additionally considered.
SLS5	Effect of small displacement modifications to the horizontal earth pressures additionally considered.
ULS1	Effect of large displacement modifications to the horizontal earth pressures (mobilizing full soil strength) additionally considered.
ULS1a	As ULS1 but with load dispersal removed.

^{iv}Note that ULS1a may produce more conservative estimates of carrying capacity than SLS4 and SLS5. It is included to allow full examination of the relative contributions of each factor.

Table 1 : Soil-structure interaction scenarios.

For the purposes of modelling each of these scenarios in RING, it is necessary to define in detail the assumed stress state on the arch extrados for each case. This requires definition of the normal and shear stresses on the extrados. For convenience the normal stress will be represented by vertical and horizontal stress components as this permits easier cross-reference to current models in the literature; these are given in Table 2. The extrados stresses due to the live load and dead load are considered here as separate and independent and as additive in terms of their effect on the arch. Justification for this and the assumptions inherent in Table 2 are detailed in §2.2, §2.3, and §2.4.

Scenario	Assumed stresses on arch extrados						
	Live load			Dead load (backfill only)			
	σ_v	σ_h	τ	σ_v	σ_h (active side)	σ_h (passive side)	τ
SLS1	$U(x)$	0	0	0	0	0	0
SLS2	$U(x)$	0	0	γz	0	0	0
SLS3	$U(x)$	0	0	γz	$K_0 \gamma z$	$K_0 \gamma z$	0
SLS4	$B(x,z)$	0	0	γz	$K_0 \gamma z$	$K_0 \gamma z$	0
SLS5	$B(x,z)$	0	0	γz	$K_a \gamma z$	γz	0
ULS1	$B(x,z)$	0	0	γz	$K_a \gamma z$	$K_e \gamma z$	0
ULS1a	$U(x)$	0	0	γz	$K_a \gamma z$	$K_e \gamma z$	0

Table 2 : Assumed interface stress states for soil-structure interaction scenarios.

In Table 2: τ is the shear stress at the interface; x is the horizontal Cartesian coordinate; z is the depth below the backfill surface; $U(x)$ is the load distribution on the backfill surface; $B(x,z)$ are the vertical components of the transformed live load $U(x)$ due to dispersal through

the backfill; γ is the unit weight of the backfill; K_0 is the at rest earth pressure coefficient; $K_a = \tan^2(45 - \phi'/2)$ is the active coefficient of lateral earth pressure; K_e is a modified passive earth pressure coefficient to be defined in §2.4.

2.2 Live loading assumptions

For small loads and negligible arch movements an elastic stress distribution (Boussinesq) may be used to estimate the increase in vertical stresses $B(x,z)$ due to the live load $U(x)$. As the load increases, initially more soil will begin to yield beneath the live load (accompanied by some minor settlement) and the distribution zone is likely to narrow in comparison to elastic theory, as shear stresses reach their limiting value. As further deformation takes place, model test kinematics (*e.g.* Fairfield & Ponniah^v) indicate that the soil moves down below the live load and then shears along the extrados away from the live load centreline.

At all loading stages, the presence of additional vertical stresses caused by the live load will clearly be the most significant in terms of pushing the arch towards failure. The horizontal stresses in the vicinity of the live load will be detrimental to the structure, but their influence will be small; the largest moment arms occur at small extrados slope angles and vice versa. Shear stresses will always act away from the centreline of the live load and are thus beneficial to the left and detrimental to the right of this when the latter is positioned at quarter span as shown in Figure 1. Due to the geometry of the mechanism, the beneficial effects of the shear stresses will normally outweigh the detrimental effects and will tend to additionally cancel out the detrimental effects of the horizontal stresses, although further studies are required to verify this.

In cases where strains are relatively small it therefore follows that the effects of the live load can be approximated reasonably well using stress increments described by a Boussinesq distribution for vertical stresses, with the horizontal and shear stresses set to zero. When strains become larger, it is expected that the vertical and horizontal stresses will decrease in the vicinity of hinge B (with the soil-arch interaction analogous to that of an inclined trapdoor). This is beneficial, as load will be shed sideways towards parts of the arch mechanism that are not displacing significantly. Further work is required to quantify the influence of this effect. For the purposes of this paper the same distribution as assumed when strains are small will be used. Though it is likely that the ‘load narrowing’ effect will be offset to some degree by the ‘load widening’ effect just discussed, in practice it may be prudent to limit the load dispersion to a greater degree as strains become very large.

2.3 SLS dead loading assumptions

SLS3 and SLS4 model the presence of the backfill and conservatively assume ‘at rest’ (zero displacement) horizontal earth pressures on both sides of the arch. The at rest earth pressure coefficient K_0 is frequently approximated by:

$$K_0 = 1 - \sin(\phi'), \quad (1)$$

where ϕ' is the angle of shearing resistance of the soil. This produces a beneficial additional

resistance on the passive side, but increases the disturbing forces on the active side. The overall effect on the arch carrying capacity is small but generally beneficial.

Small arch deformations are assumed in SLS5. As the arch begins to deform, it is expected that the vertical and horizontal stresses will increase in the vicinity of hinge C. Insights into the vertical and horizontal stress relationships may be gained by examining the investigation into retaining wall response by Terzaghi^{vi} (Figure 2). It is clear that negligible wall rotation (<0.1%) is required to vary the lateral earth pressure coefficient between K_a and 1 for dense or loose sand. A coefficient of 1 can be understood as mobilizing no soil strength, the soil effectively behaving as a dense fluid. A reasonable assumption for SLS5 is therefore $K=1$ on the passive side and $K=K_a$ on the active side.

This approach depends on the analogy between arch-soil interaction and retaining wall-soil interaction, which is not necessarily fully valid, as kinematics indicate an interaction more analogous to that of an inclined anchor on the passive side. However, regardless of the interaction mechanism, it is expected that only small deformations would be required to mobilise zero soil strength and thus achieve a loading state equivalent to that of a dense fluid.

The above discussion implies that the horizontal and vertical stresses are principal stresses and thus that consideration should be given to the shear stresses τ on the arch. These will act along the extrados away from the crown towards the springings. Thus on the loaded side these shear stresses will be beneficial, opposing collapse, whilst on the passive side, they will be detrimental, assisting collapse. However due to the position of the first and fourth hinges (labelled A on the intrados and D on the extrados in Figure 1), the beneficial action on the loaded side will outweigh the detrimental action on the passive side. It should therefore be conservative to neglect the shear stresses (*i.e.* to take these as 0).

2.4 ULS dead loading

Whilst the kinematics of the arch and soil on the passive side are more closely related to an anchor pullout, analyses in the literature tend to apply classical retaining wall theory to compute changes in the horizontal stresses. In the absence of other available solutions, the modified lateral earth pressure coefficient proposed by Burroughs et al.^{vii}, K_e is adopted:

$$K_e = K_0 + e(K_p - K_0), \quad (2)$$

where e is an empirically derived coefficient, found to lie between 0.25 and 0.45 for the model arches tested in the work, with the lower values corresponding to deeper fills. $K_p = \tan^2(45 + \phi' / 2)$ = the passive coefficient of lateral earth pressure.

The model also included a reduction in lateral stress towards the hinge located at the springing (D on Figure 1) due to low displacements at this point. However in the analysis this is likely to be a second order effect due to the low displacements in this region and hence will be ignored.

Whilst the above approach appears to work well for the range of arches on which it was calibrated, there is still significant uncertainty in its application to a wider range of scenarios. As before an assumption of $\tau = 0$ is conservative (as the shear stresses will act towards the crown and thus against the mechanism).

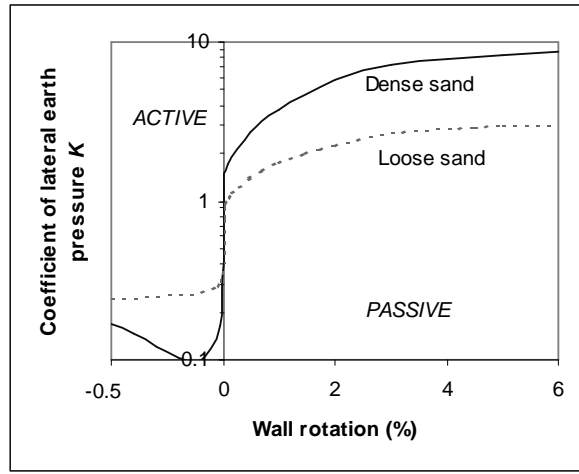


Figure 2: Relationship between earth pressure and wall rotation measured by Terzaghi for normally consolidated sand (different scales for active and passive).

3 CASE STUDY

Load deflection data^{viii} from laboratory tests on a 3m single span backfilled arch and a bare arch rib are reproduced in Figure 3, together with computed values of SLS1-5 and ULS1. The no-backfill experimental response has been scaled up for clarity. The parameters employed in the study are given in Table 3. It is clear that the arch without backfill effectively suffers a simultaneous ULS and SLS at a displacement of around 1mm (~0.1% rotation). At this stage a mechanism forms and the arch begins to lose strength. Using plastic theory this would theoretically occur at zero displacement but in reality the arch and supports have a small degree of flexibility. The largest SLS estimates, SLS4 and SLS5, correlate well with the first change in gradient of the backfilled arch load deflection curve at ~300kN, and correspond to an assumed displacement of less than 1mm (<0.1% rotation). ULS1 matches the observed ultimate load reasonably well, giving confidence in the method.

In practice it should be noted that the backfill in this experiment was compacted and would thus give rise to locked in at rest horizontal stresses in excess of those given by $K_0\sigma'_v$, an observation supported by the experimental data. This is unlikely to alter ULS1 but will have some effect on SLS3, SLS4 and SLS5 (though there is insufficient space to deal with the important issue of compacted backfills here, initial investigations indicate ‘compacted’ SLS3, SLS4, and SLS5 values will remain within approx. 10% of the values indicated on Figure 3).

4 COMPARISON OF EUROCODE 7 AND BD21 PRINCIPLES

Eurocode 7 principles require that the SLS and ULS are considered separately. The SLS calculation involves using mean soil properties, with typically no partial factors applied to the parameters. For the purposes of this paper the EC7 SLS was taken to be represented by SLS5.

The Eurocode requires two ULS cases ('B' and 'C') to be considered for the soil-arch problem. Partial factors must be applied as appropriate to characteristic values as detailed in Table 4. The live load is considered as a variable unfavourable action. It is debatable whether the net action effect of the backfill (considered as a single entity or single source) should be considered as favourable or unfavourable. In practice, this issue affects Case B only and here it will conservatively be taken as a permanent favourable action.

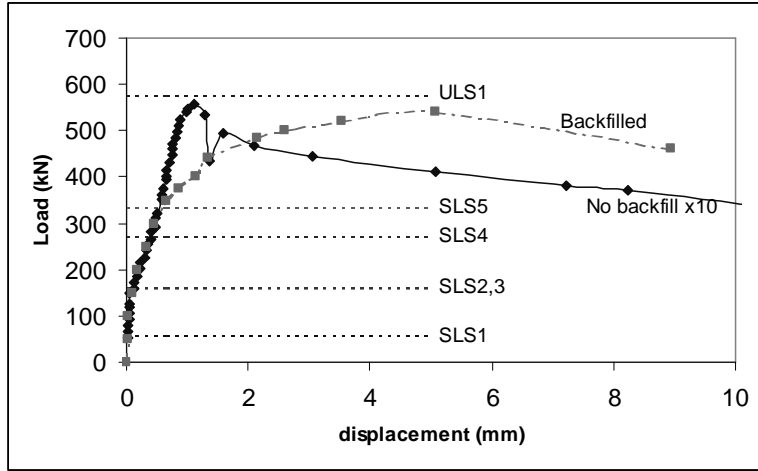


Figure 3: Experimental and predicted load vs. displacement response of single-span bridges

Parameter	Value	Parameter	Value
Width	2880mm	Masonry unit weight	22.7kN/m ³
Span	3000mm	Backfill unit weight	22.2kN/m ³
Rise	750mm	Limiting fill/barrel angle of friction	0.75φ'
Arch thickness	215mm	Loading	Boussinesq
Loading	¼ span	Limiting dispersion angle	0.75φ'
Loaded length	215mm	<i>e</i>	0.35

Table 3 : Case study parameters used in RING analysis

Case C is designed to avoid overall collapse due to failure in the soil by applying partial factors to the soil strength. In this paper Case C is taken as ULS1 divided by 1.3, where ULS1 is calculated on the basis of the factored value of $\tan\phi$. Case B is designed to avoid failure in the structure itself by applying enhanced load factors and by not factoring the soil strength. In this paper Case B is taken as ULS1 divided by 1.5.

In contrast, and in the context considered, BD21 indicates that the SLS condition effectively always governs but that this may be deemed to be satisfied provided the load does not exceed half the ULS load. This is stated to be based on examination of typical load deformation curves from full scale tests. Specifically, BD21 states that '*...it will be prudent to limit regularly applied loading, pending a detailed investigation regarding serviceability, to*

half the ultimate failure load.'. In this paper BD21 SLS will therefore be taken as ULS1 divided by 2.

Parameter	Factor	Case B	Case C
<i>Partial load factors (γ_f)</i>			
Permanent unfavourable action	γ_G	1.35	1.00
Variable unfavourable action	γ_Q	1.50	1.30
Permanent favourable action	γ_G	1.00	1.00
<i>Partial material factors (γ_m)</i>			
$\tan \phi'$	$\gamma_{\tan\phi'}$	1.00	1.25
Unit weight of ground γ	γ_g	<i>1.00</i>	<i>1.00</i>

Table 4 : Eurocode partial factors

5 PARAMETRIC STUDY

A parametric study using RING was undertaken to investigate the relationships between SLS1-5 and ULS1, 1a, and to compare the Eurocode based approach with that of BD21. The case study configuration detailed in §3 was used as the basis for the calculations and assumed angles of shearing resistances of 60° , 50° and 40° were used. For convenience the dead load coefficient of horizontal earth pressure were taken as 0 rather than K_a for SLS5 and ULS1. Studies indicated that the effect of this was minimal as the live load dominates over the dead load on this side of the arch and the passive pressures are significantly larger.

Results for $\phi'=60^\circ$ are presented in Figure 4. It can be seen that a modest increase in capacity is achieved by incorporating backfill self weight into the assessment (difference between SLS1 and SLS2). Adding in at rest horizontal pressures (SLS3) results in an almost negligible increase. Comparison of SLS4/5 and ULS1/1a show that the contribution of passive pressure resistance is roughly comparable to that of load dispersion for low depths of fill, but that load dispersal becomes more significant as the depth of fill increases. The relative magnitudes are, however, quite sensitive to the choice of load dispersal angle. Comparison of SLS4 and SLS5 indicate a modest increment in capacity for SLS5 at the point where the earth pressures through the fill on the passive side have reversed from at rest to a state of a dense fluid. In this paper, SLS5 is taken as a lower bound estimate of the EC7 SLS. However improved analysis may increase this further. In particular, the EC7 SLS may be significantly higher for very stiff fills.

In order to more clearly compare the EC7 ULS with the BD21 SLS, these values were normalized against the EC7 SLS and plotted in Figure 5 for angles of shearing resistance of 40° , 50° and 60° . Normalised values below 1 indicate a more critical limit state than the assumed EC7 SLS. It can be seen that as ϕ' reduces, the BD21 SLS begins to underestimate the EC7 SLS significantly. Whilst the EC7 ULS Case B and Case C are initially above the EC7 SLS, they drop below this for lower values of ϕ' . Thus according to EC7, stability is controlled by the SLS for higher strength backfill and the ULS for lower strength backfill (in contrast, in BD21 the SLS effectively governs throughout).

Whilst the detailed trends observed are somewhat dependent on the soil-arch interaction models adopted, it would be expected that the general trends will still be representative of those produced by more refined models. The trends still hold if the EC7 SLS is taken as the more conservative SLS4 value (this was found to be consistently 15-20% lower than SLS5 for the parameters examined).

In bridge assessment it is clearly desirable to be able to pass a bridge on a conservative estimate of the backfill strength (to avoid the expense of a detailed soil investigation). These findings show that if the BD21 approach is used when a low value of backfill strength is assumed, then it is likely to significantly underestimate the bridge capacity. If the bridge fails when using the EC7 approach (generally the ULS will be governing), a soil investigation is still beneficial as it may lead to enhanced ULS and SLS loads being computed. Further research is in progress to benchmark these findings against other bridges.

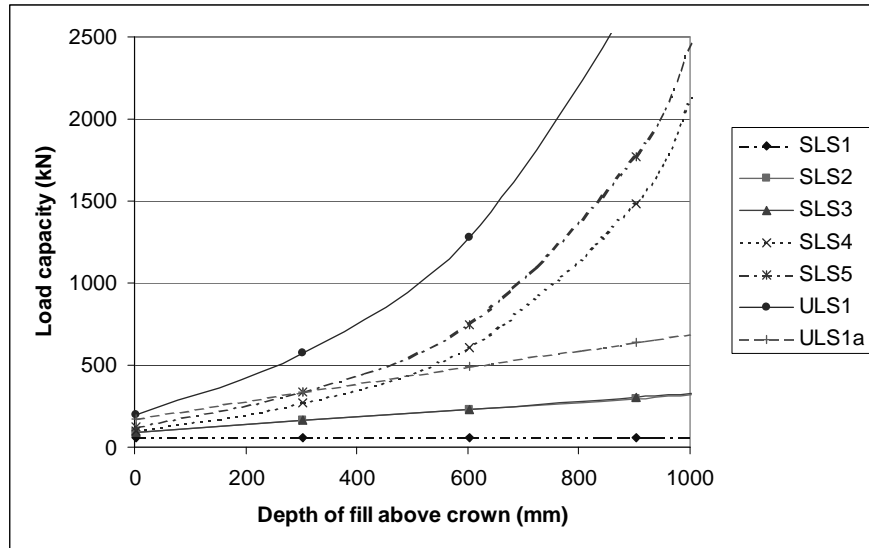


Figure 4: Variation of serviceability and ultimate limit states with depth of fill above the crown for $\phi' = 60^\circ$

6 CONCLUSIONS

- Soil-structure interaction has been discussed; further research into the load dispersal and passive resistance mechanisms are recommended.
- For an arch backfilled with dry cohesionless soil, it would appear that the contribution of load dispersal and passive pressure resistance to bridge capacity are comparable. A much smaller contribution is made by the backfill dead weight.
- A simple approach for estimating a lower bound to the serviceability limit state has been outlined and compares favourably with experimental test data.
- The application of the geotechnical Eurocode approach to masonry arch analysis has been outlined. It would appear to offer an attractive flexible assessment approach.
- The serviceability factor of 2 adopted by the UK bridge assessment standard BD21

would seem to be reasonable for bridges possessing high strength backfill but increasingly overconservative for bridges possessing lower strength fill. This in particular has implications for assessment where conservative estimates of backfill strength are made.

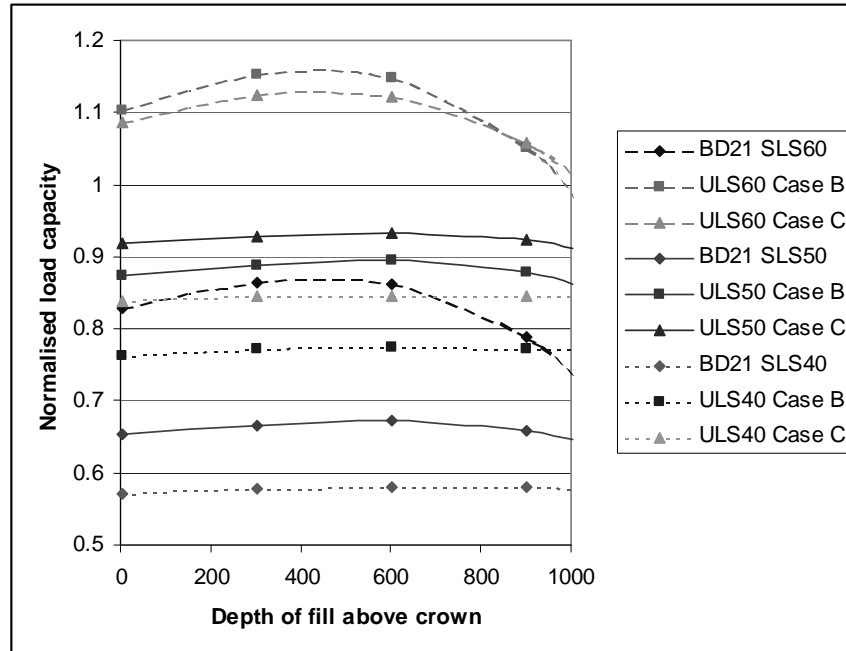


Figure 5: Variation of normalised load capacities with depth of fill above the crown. Modelled angle of shearing resistance is given in the legend after the letters SLS or ULS.

Acknowledgements: The third author is supported by an EPSRC studentship with additional sponsorship provided by Essex County Council. The opinions expressed are those of the authors.

REFERENCES

- [i] British Standards Institute. *Eurocode 7: geotechnical design. Part 1: General Rules*, BSI (1995).
- [ii] M. Gilbert, "RING: a 2D rigid-block analysis program for masonry arch bridges", in ARCH01, ed. Abdunur, C., *Proc. 3rd International Arch Bridges Conference*, Paris, 459-464 (2001).
- [iii] Department of Transport, *The assessment of Highway Bridges and Structures*, Department of Transport HMSO London (2001).
- [iv] M. Gilbert, "Gross displacement mechanism analysis of masonry bridges and tunnel linings", *Proceedings of the 11th International Brick/Block masonry conference*, Shanghai, 473-482 (1997).
- [v] C.A. Fairfield and D.A. Ponniah, "Model tests to determine the effect of fill on buried arches", *Proc. Institution of Civil Engineers, Structures and Buildings*, 104, 471-482 (1994).
- [vi] K. Terzaghi, "Anchored bulkheads". *Trans. Am. Soc. Civ. Engrs* 119, 1243-1281 (1954).
- [vii] P Burroughs, T.G. Hughes, S. Hee, M.C.R Davies. "Passive pressure development in masonry arch bridges". *Proc. Institution of Civil Engineers, Structures and Buildings* 153, 331-339 (2002)
- [viii] M. Gilbert, *The Behaviour of Masonry Arch Bridges Containing Defects*, PhD Thesis, University of Manchester (1993).